Research Article

Ocean Cooling Pattern at the Last Glacial Maximum

Kelin Zhuang[1] and John R. Giardino[2]

[1] *University of Arizona, Tucson, Arizona, AZ 85721, USA*
[2] *Texas A&M University, College Station, Texas, TX 77843, USA*

Correspondence should be addressed to Kelin Zhuang, klzhuang@hotmail.com

Ocean temperature and ocean heat content change are analyzed based on four PMIP3 model results at the Last Glacial Maximum relative to the prehistorical run. Ocean cooling mostly occurs in the upper 1000 m depth and varies spatially in the tropical and temperate zones. The Atlantic Ocean experiences greater cooling than the rest of the ocean basins. Ocean cooling is closely related to the weakening of meridional overturning circulation and enhanced intrusion of Antarctic Bottom Water into the North Atlantic.

1. Introduction

The cooling at the Last Glacial Maximum has been extensively studied geologically and numerically (e.g., [1–5]) where proxy data and numerical modeling were both employed to explore the climate sensitivity and mechanism. The Paleoclimate Modeling Intercomparison Project (PMIP2) presented large-scale features (e.g., [6]). However, the spatial pattern of cooling at that period was little studied previously. In this paper we use the newly released PMIP3 data to study the cooling pattern at the Last Glacial Maximum.

2. Methods

We analyze ocean potential temperature anomaly, ocean heat content (OHC) change, and meridional overturning mass stream function based on four available PMIP3 models of IPSL-CM5A-LR, MIROC-ESM, MPI-ESM-P, and MRI-CGCM3 so far (http://cmip-pcmdi.llnl.gov/cmip5/), which follow the PMIP3 21ka experimental design (Table 1; http://pmip3.lsce.ipsl.fr/) and make a comparison between the last 50 years of Last Glacial Maximum (LGM) experiments relative to the base period of the last 50 years of the preindustrial control run.

We calculate the temperature anomaly, meridional overturning mass stream function anomaly, and ocean heat content change of each model by regridding all the temperature data into a common $1° \times 1°$ grid.

3. Results

3.1. Geographical Distribution. Ocean cooling shows pronounced spatial variations (Figure 1), both horizontally and vertically. The Northern Hemisphere exhibits a stronger cooling than the Southern Hemisphere of IPSL-CM5A-LR, MIROC-ESM, and MPI-ESM-P except MRI-CGCM3 with stronger cooling in the Southern Ocean revealing a notable north-south asymmetry.

At the surface (Figures 1(a) and 1(b)), significant ocean cooling ($<-5°C$) occurs in the North Pacific and North Atlantic of the first three models. All these three models have shown the maximum cooling regions in the North Pacific around $40°N$ and in the Nordic Seas. But, MRI-CGCM3 demonstrates a significant cooling around $60°S$ in the Southern Ocean. It is of note that south of Greenland the model even shows a slight warming in shallow water.

At the subsurface 500 m layer (Figure 1(c)) cooling in the Pacific around $40°N$ and the North Atlantic still maintain
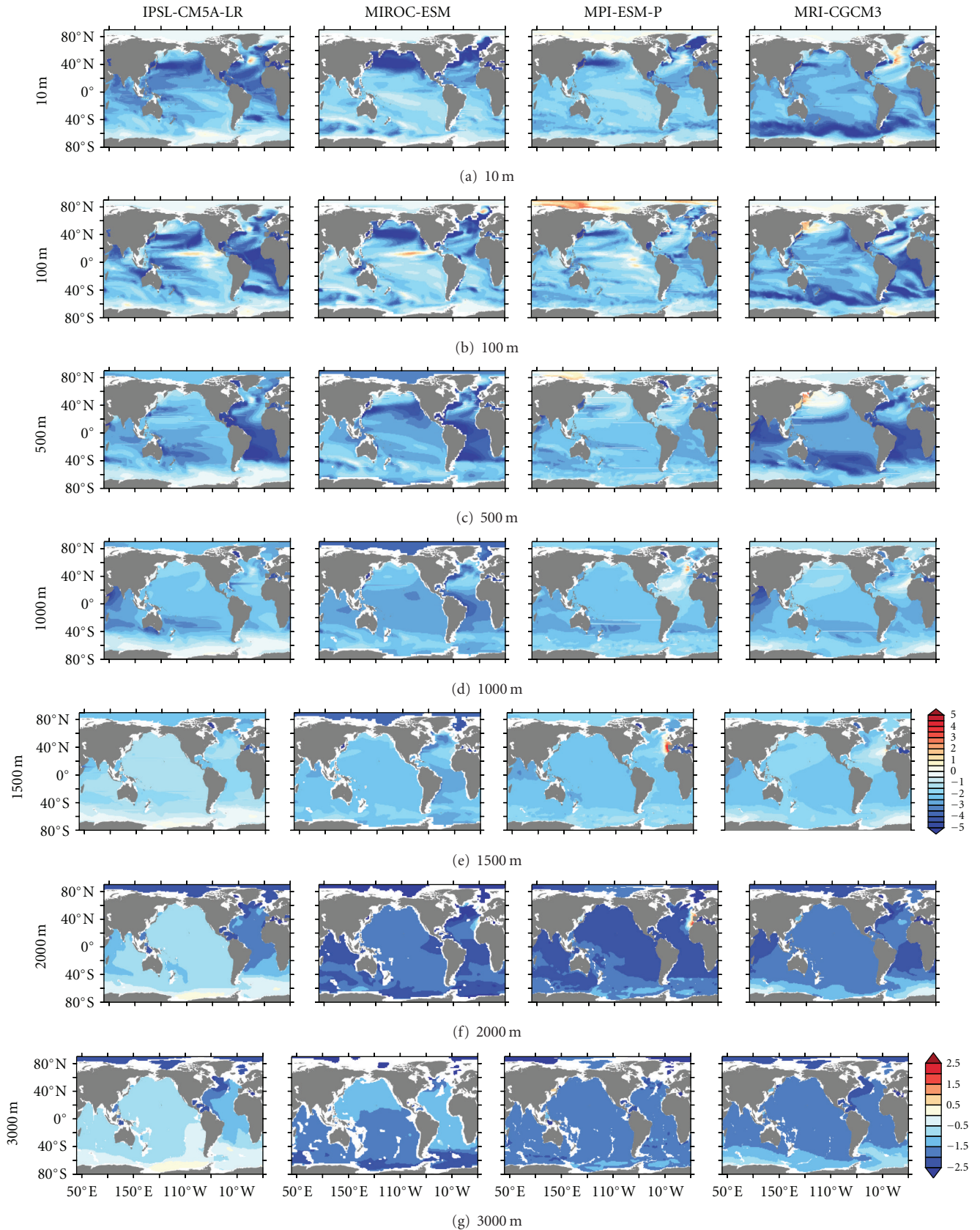
(a) 10 m

(b) 100 m

(c) 500 m

(d) 1000 m

(e) 1500 m

(f) 2000 m

(g) 3000 m

FIGURE 1: Geographical distribution of potential temperature anomaly in °C at different water depths. The abscissa is longitude in degrees and the ordinate is latitude in degrees. See text for detailed description.

TABLE 1: PMIP3 LGM models.

Model	Atmosphere	Ocean	Data output coverage
IPSL-CM5A-LR	$96 \times 95 \times L39$	$182 \times 149 \times L31$	4600–4699 (100 years)
MIROC-ESM	$128 \times 64 \times L80$	$256 \times 192 \times L44$	2501–2600 (100 years)
MPI-ESM-P	$196 \times 98 \times L47$	$256 \times 220 \times L40$	1850–1949 (100 years)
MRI-CGCM3	$320 \times 160 \times L48$	$364 \times 368 \times L51$	2501–2600 (100 years)

TABLE 2: Ocean heat content change ($\times 10^{24}$ J).

	Whole water depth				0–2000 m			
	IPSL	MIROC	MPI	MRI	IPSL	MIROC	MPI	MRI
Global	−7.39	−9.96	−10.70	−11.25	−5.43	−6.08	−5.78	−6.32
Atlantic	−1.88	−1.88	−1.86	−2.23	−1.31	−1.32	−0.94	−1.27
Arctic	−0.14	−0.13	−0.10	−0.08	−0.09	−0.09	−0.07	−0.04
Pacific	−2.78	−4.08	−4.41	−4.59	−2.04	−2.46	−2.30	−2.33
Indian	−1.08	−1.18	−1.45	−1.58	−0.82	−0.72	−0.82	−0.96
Southern	−1.31	−2.72	−2.69	−2.60	−0.98	−1.47	−1.46	−1.56

the surface cooling pattern. However, the South Atlantic demonstrates the strongest cooling in IPSL, MIROC, and MRI models. Strong cooling in the Indian and Southern Oceans is also presented in the MRI model.

The water body between 1000–2000 m experiences a moderate cooling of −2°C (Figures 1(d), 1(e) and 1(f)). All the four models have shown that north of the Gulf Stream region and South Atlantic experience more significant cooling than the rest of the regions. The Southern Ocean around 40°S has a larger amount of cooling as well. It is of note that the eastern boundary of the North Atlantic shows the slightest cooling and even warming in the MPI model.

The four models differ remarkably below 2000 m (Figures 1(f) and 1(g)). The IPSL model only shows a cooling of about −1.0°C in the large expanse with a maximum cooling of −2.5°C south of the Greenland whilst the Southern Ocean shows merely slight cooling. But, the other three models of MIROC, MPI, and MRI show a much stronger cooling of greater than −2°C. The MIROC shows the strongest cooling in the Southern Ocean. But, MRI shows strong cooling in the Indian and Southern Oceans.

3.2. Latitudinal Cross Sections and Depth Variations. Figure 2 reveals that large cooling occurs in the upper 1000 m. The temperate and tropical zones between 40°S–40°N are marked by subsurface cooling. The northern high latitude north of 40°N experiences maximum surface cooling. It is of note that the deep Arctic Ocean experiences the largest cooling in MIROC and MRI whereas IPSL and MPI only show merely a subsurface cooling.

Ocean basins act differently. The cooling in the Atlantic (Figure 2(b)) penetrates to 3000 m with a strikingly subsurface cooling center between 20°S and 20°N. 40°N–70°N shows a surface cooling.

Compared to the Atlantic and Arctic, the Pacific, and Indian demonstrate a shallower cooling. All four models show a maximum cooling around 40°N. However, the cooling only penetrates to 600 m in IPSL and MPI, but the other two models have a deeper penetration depth.

Profiles of temperature anomaly in different ocean basins indicate that the largest surface cooling occurs in the North Atlantic (Figure 3). IPSL and MRI show a global average cooling of −2.5°C whilst MIROC and MPI have a cooling of −2°C. The North and South Atlantic in IPSL and MIROC show a similar pattern with a maximum of −5°C at 400−500 m. The Arctic cooling has a similar pattern in the four models where the coolest zone lies in the deep ocean. The other basins all exhibit a rapid subsurface cooling variation in the upper ocean.

3.3. Ocean Heat Content. Ocean heat content (OHC) change reveals the integrated cooling. Figure 4 reveals the OHC change of the four models. The IPSL model shows most cooling happens in the Atlantic, parts of the Pacific and Indian. But MIROC, MPI, and MRI models demonstrate a much more significant cooling in the Pacific and Indian. Figure 5 lists the average and total OHC change. The North Pacific and Southern Ocean have the strongest change of average OHC.

More than half of OHC change occurs above 2000 m. Like temperature change in oceans, OHC change also takes place mainly in the upper ocean to 2000 m (Table 2). On a global scale, the upper 2000 m accounts for 73%, 61%, 54%, and 56% in IPSL, MIROC, MPI, and MRI, respectively.

OHC change has its individual feature in the five Ocean basins. The OHC change in Atlantic, Arctic, and Indian is almost the same for the four models but differs in the North Pacific and Southern Ocean, which also affect the total OHC

(a) Global

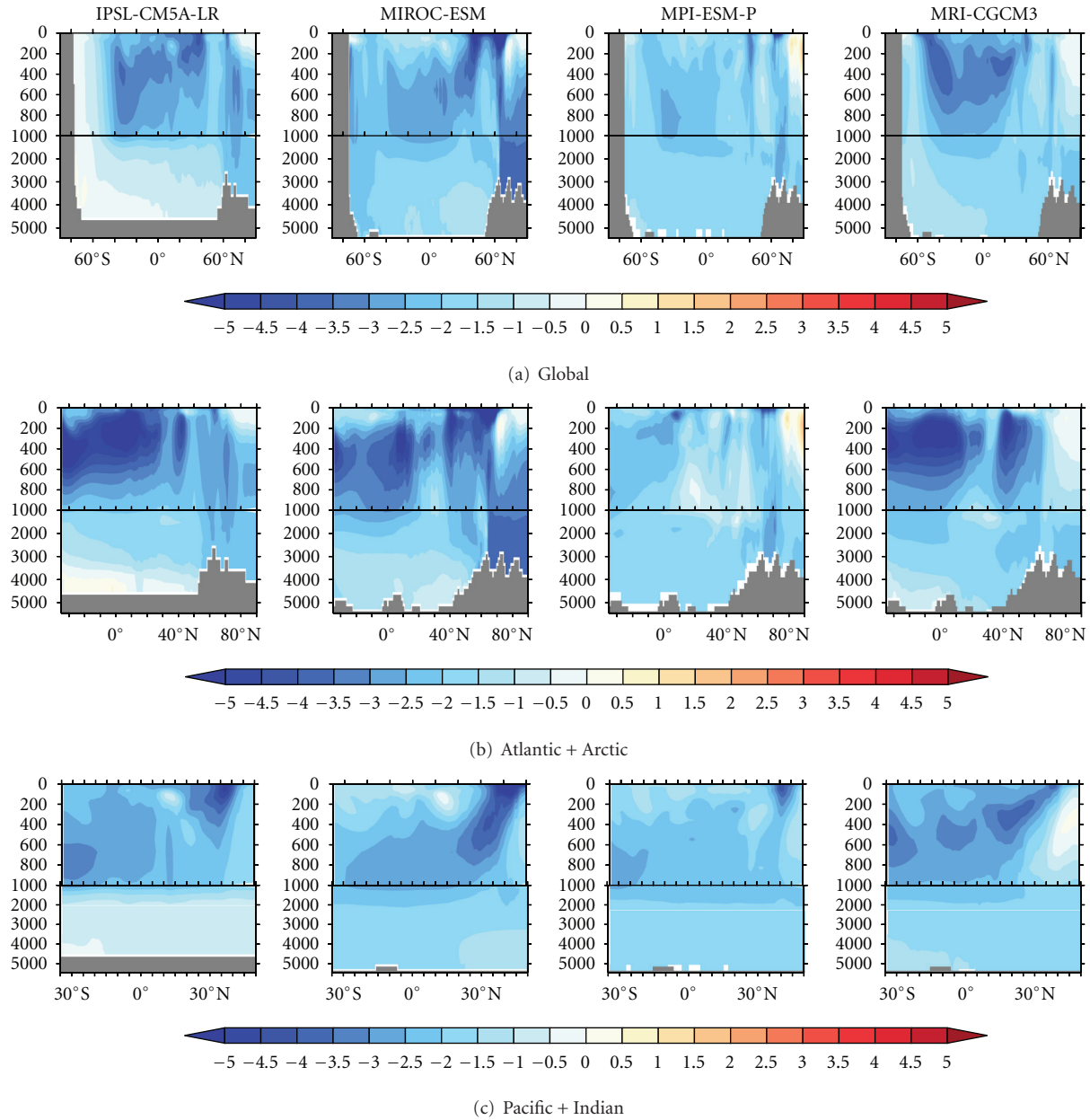
(b) Atlantic + Arctic

(c) Pacific + Indian

FIGURE 2: Latitudinal cross-sections of global mean (a) and ocean basins (b through c). The abscissa is latitude in degrees and the ordinate is water depth in meters. Notice that depth is unevenly distributed. The temperature anomaly is in °C. Cooling occurs mostly in the upper ocean. Cooling in the Atlantic and Arctic Oceans is deeper than in the Pacific and Indian Oceans.

change (Figure 5(b)). It is of note that the 2000 m OHC change is similar for all the four models and, therefore, the OHC change difference in the Pacific and Southern Ocean lies in the deep ocean.

4. Discussions

Unfortunately, not all PMIP3 models output ocean meridional overturning mass stream function. Among the four released model results, only MPI and MRI have meridional

overturning variables. Meridional overturning circulation (MOC) changes are usually the responses to climate change. Here we explore the links between the MOC change and temperature anomaly on the global scale and regional scale at the Last Glacial Maximum.

Previous studies have revealed that cooling at the Last Glacial Maximum is closely related to meridional overturning circulation (MOC) [7–9]. They simulated a shallower and weaker North Atlantic Deep Water circulation and an enhanced intrusion of Antarctic Bottom Water (AABW) into

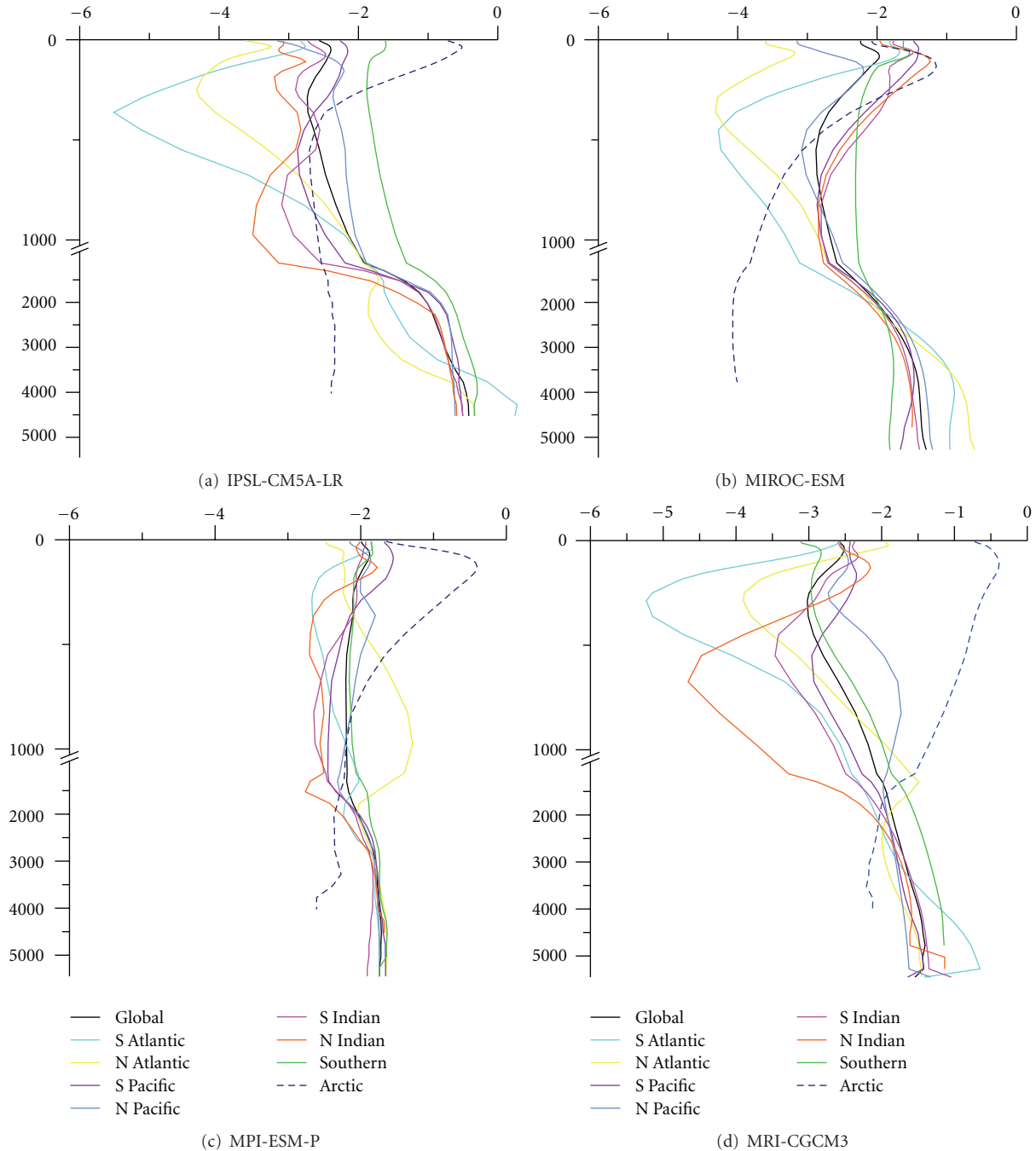(a) IPSL-CM5A-LR

(b) MIROC-ESM

(c) MPI-ESM-P

(d) MRI-CGCM3

FIGURE 3: Ocean cooling profiles of global mean and ocean basins. The abscissa is temperature anomaly in °C and the ordinate is water depth in m. The maximum surface warming occurs in the North Atlantic. Ocean cooling mostly concentrates in the upper 1000 m with rapid variations in different basins.

the North Atlantic [10]. Ganopolski and Rahmstorf [8] proposed a cold mode MOC to explain the cooling mechanism at the Last Glacial Maximum.

On a global scale the upper 2000 m witnesses a weakening trend of the MOC although the magnitude varies in the two models (Figure 6(a)). MPI presents a negative MOC anomaly whilst MRI only shows a slight decrease of MOC compared to the preindustrial run. In the deep part we can

observe the enhancement of AABM. Both models exhibit the weakening of the Atlantic meridional overturning circulation (Figure 6(b)). Figures 1 and 2 have different temperature distributions with regard to MPI and MRI. Cooling in the upper Pacific and Indian Oceans simulated by MPI is not as strong as cooling by MRI, which is closely related to the enhanced MOC change in MPI upper ocean while MRI upper part shows a weakening MOC change.
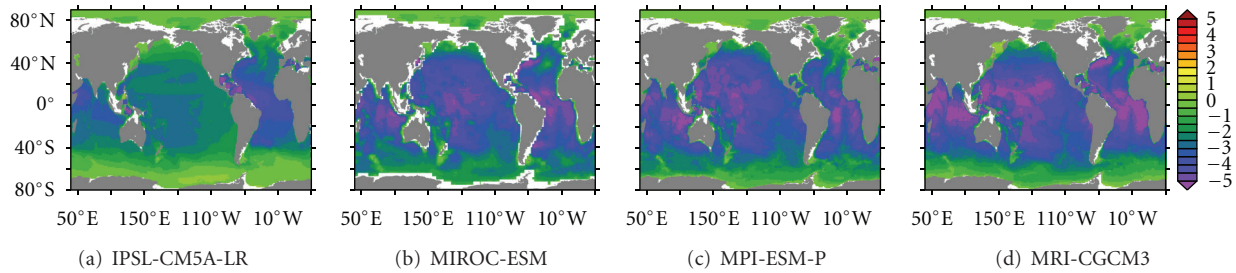
(a) IPSL-CM5A-LR   (b) MIROC-ESM   (c) MPI-ESM-P   (d) MRI-CGCM3

FIGURE 4: Ocean heat content change ($\times 10^{10}$ Jm^{-2}) at the Last Glacial Maximum. Most cooling occurs between 40°S and 40°N. All the four models show cooling in the Atlantic. But, cooling in the Pacific and Indian Oceans varies.
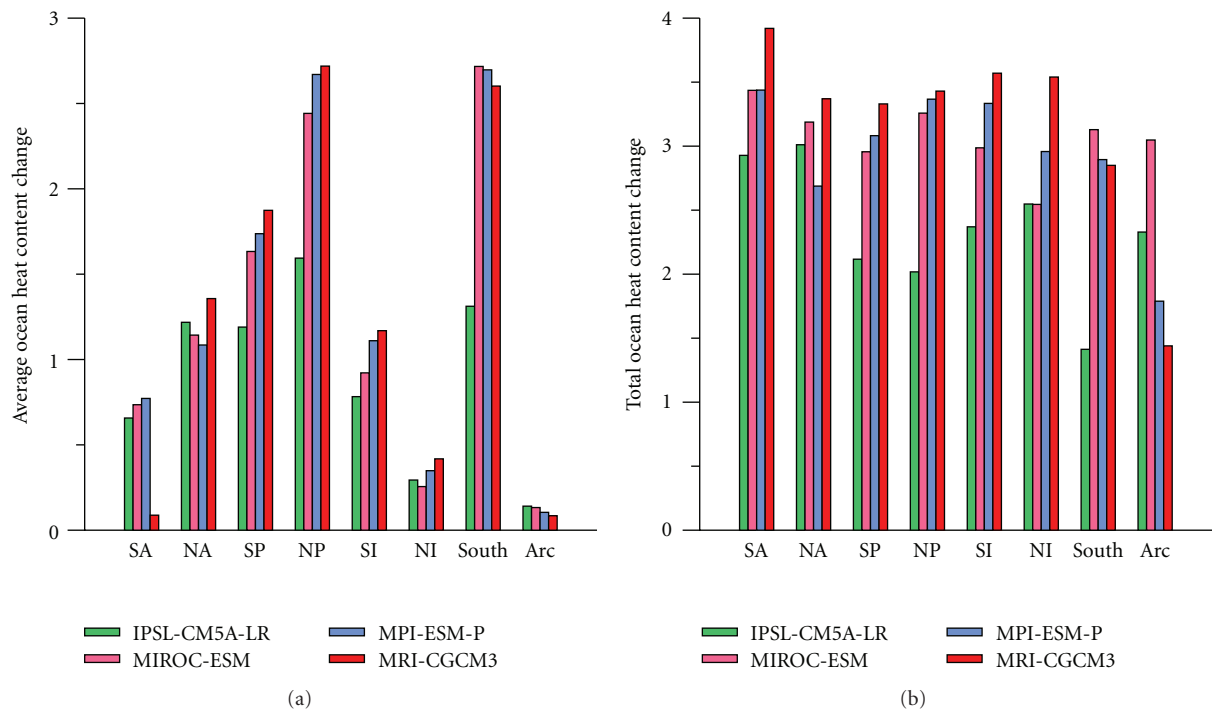

(a)

(b)

FIGURE 5: Ocean heat content change in ocean basins. (a) Average OHC change ($\times 10^{10}$ Jm^{-2}) and (b) total OHC change ($\times 10^{24}$ J). Cooling in the North Pacific and Southern Ocean differs in magnitude among the four models. SA—South Atlantic, NA—North Atlantic, SP—South Pacific, NP—North Pacific, SI—South Indian, NI—North Indian, South—Southern Ocean, Arc—Arctic.

Based on the MOC change and temperature anomaly in these two models, we can see that weakening of MOC in the upper ocean is closely related to upper cooling and enhancement of AABW in the deep part is associated with cooling in the deep ocean.

5. Summaries

Although the four models differ in cooling magnitude, we see that cooling at the Last Glacial Maximum varies both horizontally and vertically. Cooling mostly occurs between 40°S and 40°N in the upper 1000 m. More than half of OHC change happens in the upper 2000 m.

All the four models are in agreement that ocean basins, except the Arctic, are featured by surface to subsurface cooling. Cooling in the Atlantic and Arctic is much deeper than the Pacific and Indian. The Atlantic experiences the greatest cooling at the Last Glacial Maximum. Ocean cooling at the Last Glacial Maximum is closely related to the MOC change.

Acknowledgments

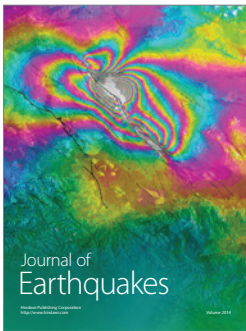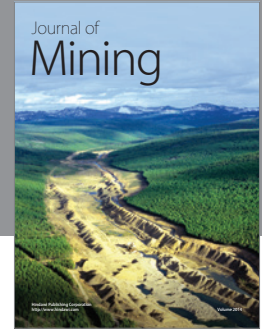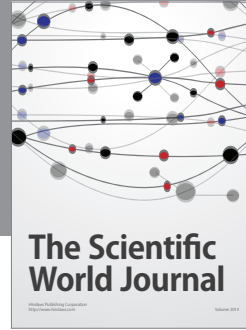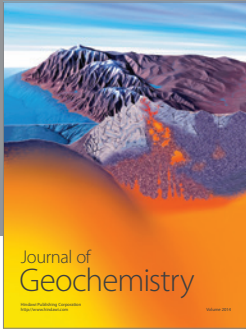(a) Global

(b) Atlantic + Arctic

(c) Pacific + Indian
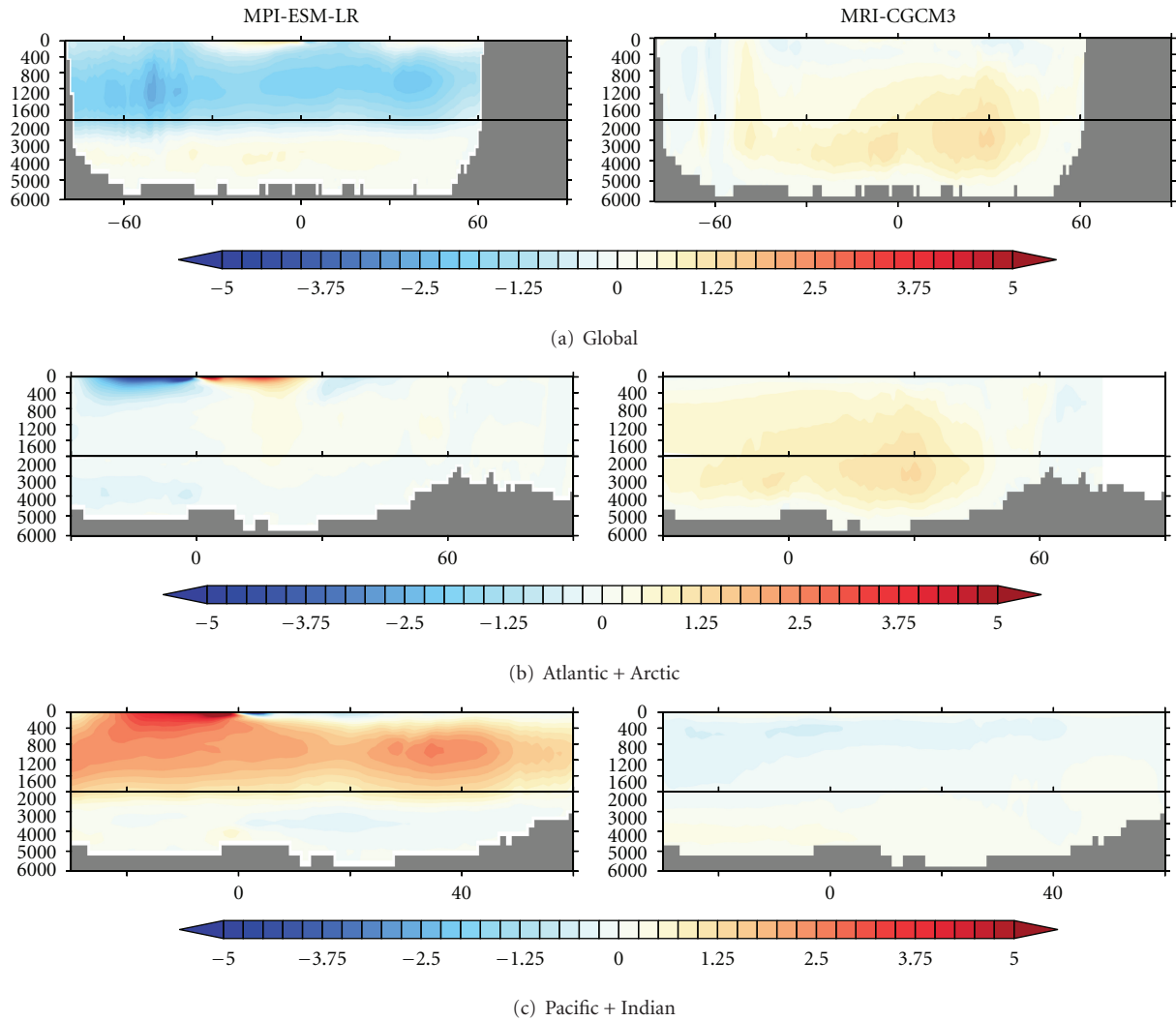
FIGURE 6: Ocean meridional overturning mass-stream function anomaly of global mean (a) and ocean basins (b through c). The abscissa is latitude in degrees and the ordinate is water depth in meters. Notice that depth is unevenly distributed. The overturning mass-stream function anomaly is in $\times 10^{10}$ kg s^{-1}. MOC weakens in the upper ocean whereas the AABW is enhanced. It is of note that MOC change in the Pacific and Indian Oceans are different in MPI and MRI.

References

[1] A. Schmittner, N. M. Urban, J. D. Shakun et al., "Climate sensitivity estimated from temperature reconstructions of the Last Glacial Maximum," *Science*, vol. 334, pp. 1385–1388, 2011.

[2] Y. Okazaki, A. Timmermann, L. Menviel et al., "Deepwater formation in the North Pacific during the last glacial termination," *Science*, vol. 329, no. 5988, pp. 200–204, 2010.

[3] MARGO Project Members, "Constraints on the magnitude and patterns of ocean cooling at the Last Glacial Maximum," *Nature Geoscience*, vol. 2, pp. 127–132, 2009.

[4] M. Kageyama, A. Laîné, A. Abe-Ouchi et al., "Last Glacial Maximum temperatures over the North Atlantic, Europe and western Siberia: a comparison between PMIP models, MARGO sea-surface temperatures and pollen-based reconstructions," *Quaternary Science Reviews*, vol. 25, no. 17-18, pp. 2082–2102, 2006.

[5] A. J. Weaver, M. Eby, A. F. Fanning, and E. C. Wiebe, "Simulated influence of carbon dioxide, orbital forcing and ice sheets on the climate of the Last Glacial Maximum," *Nature*, vol. 394, no. 6696, pp. 847–853, 1998.

[6] P. Braconnot, B. Otto-Bliesner, S. Harrison et al., "Results of PMIP2 coupled simulations of the Mid-Holocene and last glacial maximum—part 1: experiments and large-scale features," *Climate of the Past*, vol. 3, no. 2, pp. 261–277, 2007.

[7] A. Ganopolski, S. Rahmstorf, V. Petoukhov, and M. Claussen, "Simulation of modern and glacial climates with a coupled global model of intermediate complexity," *Nature*, vol. 391, no. 6665, pp. 351–356, 1998.

[8] A. Ganopolski and S. Rahmstorf, "Rapid changes of glacial climate simulated in a coupled climate model," *Nature*, vol. 409, no. 6817, pp. 153–158, 2001.

[9] A. F. Thompson and S. Rahmstorf, "Ocean circulation," in *Surface Ocean—Lower Atmosphere Processes*, C. L. Quere and E. S. Saltzman, Eds., Geographical Monograph 187, pp. 99–118, American Geophysical Union, 2009.

[10] S. I. Shin, Z. Liu, B. L. Otto-Bliesner, J. E. Kutzbach, and S. J. Vavrus, "Southern Ocean sea-ice control of the glacial North Atlantic thermohaline circulation," *Geophysical Research Letters*, vol. 30, no. 2, pp. 68–1, 2003.